Food Chemistry 291 (2019) 94–100

Contents lists available at ScienceDirect

Food Chemistry

journal homepage: www.elsevier.com/locate/foodchem

# Hydration shells of carbohydrate polymers studied by calorimetry and terahertz spectroscopy

Jose Antonio Morales-Hernández[a], Abhishek K. Singh[b], Socorro Josefina Villanueva-Rodriguez[a], Enrique Castro-Camus[b,*]

[a] Centro de Investigación y Asistencia en Tecnología y Diseño del Estado de Jalisco, A.C., Avenida Normalistas 800, Colonia Colinas de la Normal, Guadalajara 44270, JAL, Mexico
[b] Centro de Investigaciones en Optica, A.C. Loma del Bosque 115, Lomas del Campestre, Leon, Guanajuato 37150, Mexico

ARTICLE INFO

*Keywords:*
Terahertz spectroscopy
Calorimetry
Aqueous solutions
Hydration shell
Agave fructans
Inulin

ABSTRACT

We present a study of the hydration shells of some carbohydrate polymers of commercial and biological importance, namely, agave fructans, inulin, and maltodextrin, employing terahertz time-domain spectroscopy and differential scanning calorimetry. We observe that the hydration numbers calculated using terahertz spectroscopy are marginally higher than those of the calorimetric values. We attribute this discrepancy to the definition of hydration number, which in a way correlates with the physical process used to quantify it. The aqueous solutions show a non-proportional increase in the absorption coefficient and the hydration number, with a decrease in the carbohydrate concentration. We demonstrate that this behavior is consistent with the "chaotropic" or "structure breaking" model of the hydration shell around the carbohydrates. In addition, the study reveals that agave fructans and inulin have good hydration ability. Given the high glass transition temperature and good hydration ability, these carbohydrates may behave as good bio-protectants and hydrating additives for food and beverages.

## 1. Introduction

The protective effect against freezing and dehydration of carbohydrates on biomolecules has been a subject of great interest in the area of cryopreservation and biomedical research (Jain & Roy, 2009). It is believed that water molecules are transiently linked to their neighboring water molecules via a fluctuating local tetrahedral network of hydrogen bonds at ambient conditions (Cipcigan, Sokhan, Martyna, & Crain, 2018; Head-Gordon & Johnson, 2006). However, when macromolecules like carbohydrates, peptides, proteins, etc. are dissolved in water, the structural tetrahedral network is perturbed in the vicinity of a solute macromolecule (Sajadi et al., 2014; Ebbinghaus et al., 2007; Heugen et al., 2006; Shiraga, Ogawa, Kondo, Irisawa, & Imamura, 2013; Shiraga et al., 2017). In the literature, such H-bond water network perturbations are referred to as hydration dynamics. The timescales for the dynamics of water molecules affected by the presence of a macromolecule fall in the sub-picosecond region (i.e., terahertz frequencies). Terahertz spectroscopy has emerged as an innovative and sensitive tool in recent decades to shine light onto the intermolecular water network around macromolecular solutes. Recently, a number of such studies on the hydration dynamics of mono- and disaccharides employing terahertz absorption and reflection spectroscopy have appeared (Singh, Morales, Estrada, Rodriguez, & Castro-Camus, 2018; Heugen et al., 2006; Shiraga et al., 2013, 2017; Sajadi, Ajaj, Ioffe, Weingärtner, & Ernsting, 2010; Shiraga, Suzuki, Kondo, De Baerdemaeker, & Ogawa, 2015; Charkhesht, Regmi, Mitchell-Koch, Cheng, & Vinh, 2018; Born, Kim, Ebbinghaus, Gruebele, & Havenith, 2009; Lipps, Levy, & Markelz, 2012). However, terahertz absorption spectroscopy is relatively hard to implement because water shows strong absorption at terahertz frequencies (Beard, Turner, & Schmuttenmaer, 2002), limiting its applicability at high water concentration. A promising alternative is terahertz spectroscopy in an attenuated total reflection (ATR) configuration which we employed in this work.

In this paper, we present a study of the hydration dynamics of aqueous solutions of carbohydrate polymers employing terahertz spectroscopy and differential scanning calorimetry. The carbohydrates under study in the current investigation are agave fructans, inulin, and maltodextrin. Currently, the major source of agave fructans is *Agave tequilana*, endemic to the states of Aguascalientes, Jalisco, Colima, Nayarit and others, in Mexico, inulin can be extracted from garlic, onions, bananas, wheat, asparagus, chicory among others, and

* Corresponding author.
*E-mail address:* enrique@cio.mx (E. Castro-Camus).

https://doi.org/10.1016/j.foodchem.2019.03.132
Received 29 January 2019; Received in revised form 21 March 2019; Accepted 25 March 2019
Available online 26 March 2019

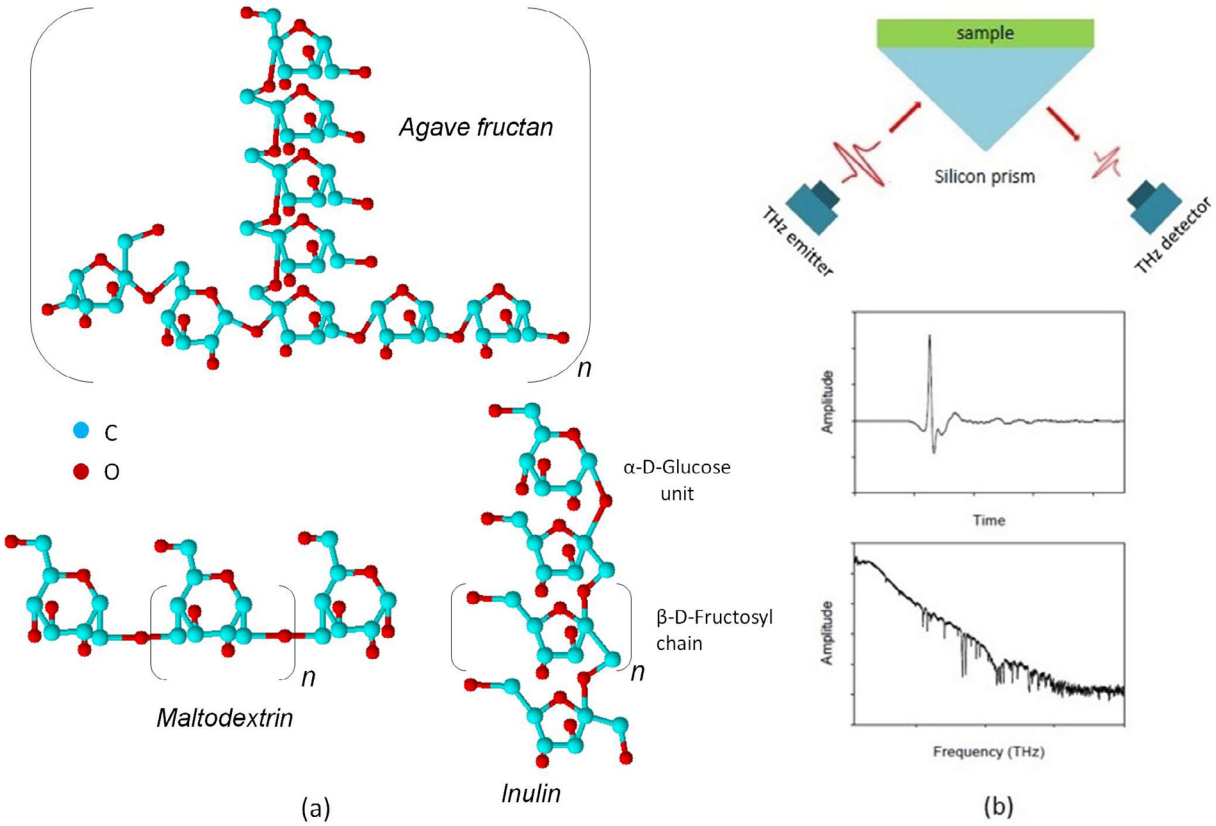


**Fig. 1.** (a) Molecular structure of agave fructans, inulin, and maltodextrin; (b) Schematic representation of the THz set-up in ATR configuration (top). The qualitative THz pulse in the time domain and the corresponding spectrum in the frequency domain are also shown (bottom).

maltodextrin can be enzymatically derived from any starch. Carbohydrates such as agave fructans and inulin are believed to be more advantageous alternatives as hydrating additives as compared to conventional carbohydrates used nowadays, given their health benefits (Contreras-Haro et al., 2017; López-Romero, Ayala-Zavala, González-Aguilar, Peña-Ramos, & González-Ríos, 2017; García-Vieyra, Del Real, & López, 2014). These carbohydrates are considered to be bioactive materials showing antifungal, antioxidant, antihypertensive, antiparasitic and anticancer activity (López-Romero et al., 2017). The use of these carbohydrates as additives in food and drinks is supposed to help in preventing osteoporosis by increasing calcium absorption (García-Vieyra et al., 2014), stimulate the immune system (García-Vieyra et al., 2014), reduce constipation and risk of colon cancer (López-Romero et al., 2017; García-Vieyra et al., 2014), and decrease diseases caused by bacteria in the intestine (García-Vieyra et al., 2014). In addition, these carbohydrates are effectively resistant to human digestive enzymes, and therefore, do not increase the sugar level in the blood, preventing obesity and other conditions (Contreras-Haro et al., 2017; Sáyago-Ayerdi et al., 2014). Because of these health benefits, it is desirable to use these carbohydrates as additives in food and beverages. Therefore, it is important to have a clear picture of the hydration ability of these carbohydrates. For example, among all the disaccharides, trehalose is believed to be very effective bio-protectant and hydration agent. This has been proved by studying the hydration dynamics (Jain & Roy, 2009; Magno & Gallo, 2011; Guo, Puhlev, Brown, Mansbridge, & Levine, 2000; Sajadi et al., 2014, 2017; Shiraga et al., 2015).

In this study, these carbohydrates reveal relatively high hydration numbers per solute molecule as compared to mono- and disaccharides. The high hydration number reveals that the carbohydrates under consideration influence the water structure and dynamics much more effectively, and hence, are expected to be more appropriate for hindering crystallization. Previously, hydration dynamics in aqueous solutions of carbohydrates and proteins has widely been studied using various experimental techniques such as compressibility measurements (Galema & Hoeiland, 1991), viscometry (Branca et al., 2001), calorimetriy (Furuki, 2002), depolarized light scattering (Rossi et al., 2011), NMR spectroscopy (Engelsen, Herve du Penhoat, & Perez, 1995), THz spectroscopy (Heugen et al., 2006; Shiraga et al., 2013, 2017; Born et al., 2009, Lipps et al., 2012, Knab, Chen, & Markelz, 2006), as well as molecular dynamics simulation. In particular, NMR, depolarised light scattering, and THz spectroscopy probe the real-time hydration dynamics. However, there is wide disagreement between the hydration numbers per solute carbohydrate molecule calculated using the different experimental approaches, because of their different definitions for hydration number. Here, we employ calorimetric and terahertz spectroscopy to undertake the investigation of aqueous solutions of carbohydrates, focusing on the differences in the hydration numbers calculated from the two techniques.

## 2. Materials and methods

Commercial agave fructans (FAC), with an average degree of polymerization around 18, were purchased from “The iidea company” (Inufib, Jalisco, Mexico). Inulin (I), with an average degree of polymerization around 14, was purchased from Orafti (Inulin GR, Tienen, Belgium). Maltodextrin-DE20 (M), with an average degree of polymerization around 6, was purchased from Habacuq company (Jalisco, Mexico). The molecular structures of the carbohydrates are shown in Fig. 1(a). The as-received samples of commercial agave fructans (FAC) contained around 6% of fructose and less than 1% of sucrose and glucose as impurities, and they were purified to get purified agave fructans (FAP) with less than 0.5% of mono- and disaccharide impurities, as reported by Moreno-Vilet, Bostyn, Flores-Montano, and Camacho-Ruiz (2017). The inulin samples contained 5.1% of sucrose as major

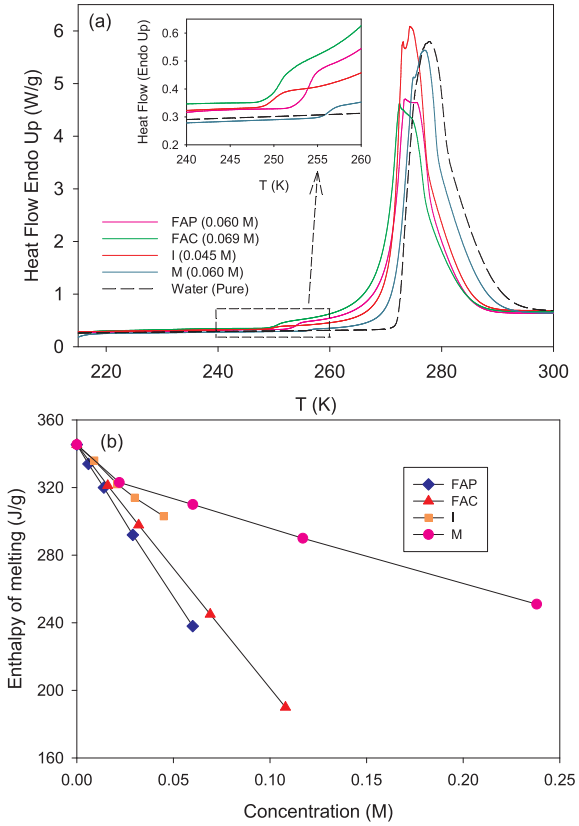


**Fig. 2.** (a) DSC scans for carbohydrate solutions. The samples were supercooled from room temperature to 200 K followed by subsequent heating. The endotherms around 273 K correspond to melting of the frozen water content. The inset shows the magnified view of the glass transition events due to a fraction of the solution transformed into the amorphous phase during supercooling. (b) Variation of enthalpy of melting of bulk (or freezable) water content with solute concentration the solution. The abbreviations FAP, FAC, I and M are used for purified agave fructans, commercial agave fructans, inulin and maltodextrin, respectively. The solid lines are "guides to eye".

impurity, whereas, maltodextrin contained around 9% of glucose. The inulin and maltodextrin samples were used as-received, without any further purification. The average degree of polymerization of the purified agave fructans is around 22. The average degree of polymerization is significant since the carbohydrates studied are a mixture of mono-, di-, oligo-, and poly-saccharides with different degrees of polymerization. In order to calculate the molar concentrations, the average degree of polymerization is required. The solubility of carbohydrates in water was determined as per method reported by Cardoso, Carvalho, and Sabadini (2012). Initially, 5 mL of the aqueous solutions of carbohydrates of different concentrations were prepared with excess of the solutes, in order to obtain supersaturated solutions (precipitate observation). The samples were prepared at constant stirring (400 rpm) for 30 minutes followed by centrifugation at 2770 × g (4000 rpm) (Centrifuge TDL-40B, Luzeren). Thereafter, samples from the supernatant were measured using a refractometer (digital refractometer, ABBE MARK II, Reichert-Jung, Massachusetts, USA) in order to determine the carbohydrate concentration in the equilibrium phase. The average of three such measurements was taken to determine the solubility. The measured solubility limit of the carbohydrates FAC, FAP, I, and M are 40.27, 31.4, 34.6, and 13.8, respectively, in $g_{solute}/100g_{water}$ at 25 °C. The aqueous solutions were prepared at two concentrations well below, and two concentrations close to the solubility limit. Typical powder samples were dissolved in deionized water, without any further purification, using a vortex for 2 min and letting all the solutions rest for 24 hours at 25 °C.

### 2.1. Differential scanning calorimetry (DSC)

For calorimetric measurements, we used a DSC Q2000 TA-Instruments (DE, USA). The measurements were performed using aluminum hermetic pans from TA Instruments. All the measurements were performed at a cooling/heating rate of 10 °/min. An empty aluminum hermetic pan was used as a reference. The DSC was calibrated for temperature using indium and distilled water as standard references. The sample chamber was purged with nitrogen gas at a flow rate of 50 mL/min. The data was analyzed using Universal Analysis 2000 software, version 4.7a (TA Instruments, New Castle, USA).

### 2.2. Terahertz time-domain spectroscopy (TDS)

An API TeraGauge terahertz time-domain spectrometer was used to produce and detect THz pulses with a bandwidth of ~2 THz. The system was configured in an attenuated total reflection geometry by incorporating a Si prism (Soltani et al., 2016). This technique has recently attracted significant attention to study highly absorbing liquids such as water and aqueous solutions in the terahertz frequency region. The schematic representation of the TDS-THz setup in an ATR configuration is shown in Fig. 1(b). We placed the Si prism (n = 4.2) at the focal position of the THz waves emerging from the emitter. The incidence angle of the THz pulse at the prism surface (prism-liquid interface) was 45 deg. We used TE - polarization geometry to probe the hydration driven changes in the complex refractive index of our solutions.

## 3. Results and discussion

### 3.1. DSC measurements

Water present in the aqueous solutions of carbohydrates may be classified into two categories; freezable, namely, bulk water with a structural tetrahedral network, and non-freezable, with a distorted H-bond network owing to the influence of the carbohydrate molecules. The water molecules bound to the carbohydrate exist in an amorphous state and they do not crystallize while the solution is being supercooled. In our measurements, we supercool the aqueous solutions up to around 200 K, a sufficiently low temperature for bulk water to crystallize. The bulk water present in the solution crystallizes, and the water in the hydration sphere gets supercooled. With subsequent heating, the crystallized bulk water melts at around 273 K, as shown in Fig. 2(a). The freezable water content can be measured by calculating enthalpy of the melting endotherm. With increasing carbohydrate concentration in the solution, the melting enthalpy continuously decreases given reduction in the fraction of freezable water content in the solution, as shown in Fig. 2(b). The amount of non-freezable water is related to the hydration water in the solution at that particular concentration. The quantitative assessment of the hydration sphere around the solute carbohydrate molecule can be estimated by calculating the hydration number. Here, we calculate the hydration number as a ratio of mole fraction of non-freezable water (or hydration water) to the mole fraction of sugar concentration in the aqueous solution, at each concentration studied.

### 3.2. THz-ATR measurements

The spectroscopic region, in which the present study is performed, lies between 0.3 THz to 2 THz, which corresponds to the frequency region between the slow relaxation mode of water at low frequencies and the fast vibrational and librational contributions at high frequencies (Shiraga et al., 2017). In Fig. 3(a), (b), (c) and (d), we show the real ($n$) and imaginary ($\kappa$) parts of the complex refractive index, extracted from THz-TDS data for all the carbohydrates studied here with varying concentrations, in the frequency range of 0.3–2 THz. As shown in the figure, for all the samples, both the real and imaginary parts of the complex refractive index show a monotonous decrease with increasing

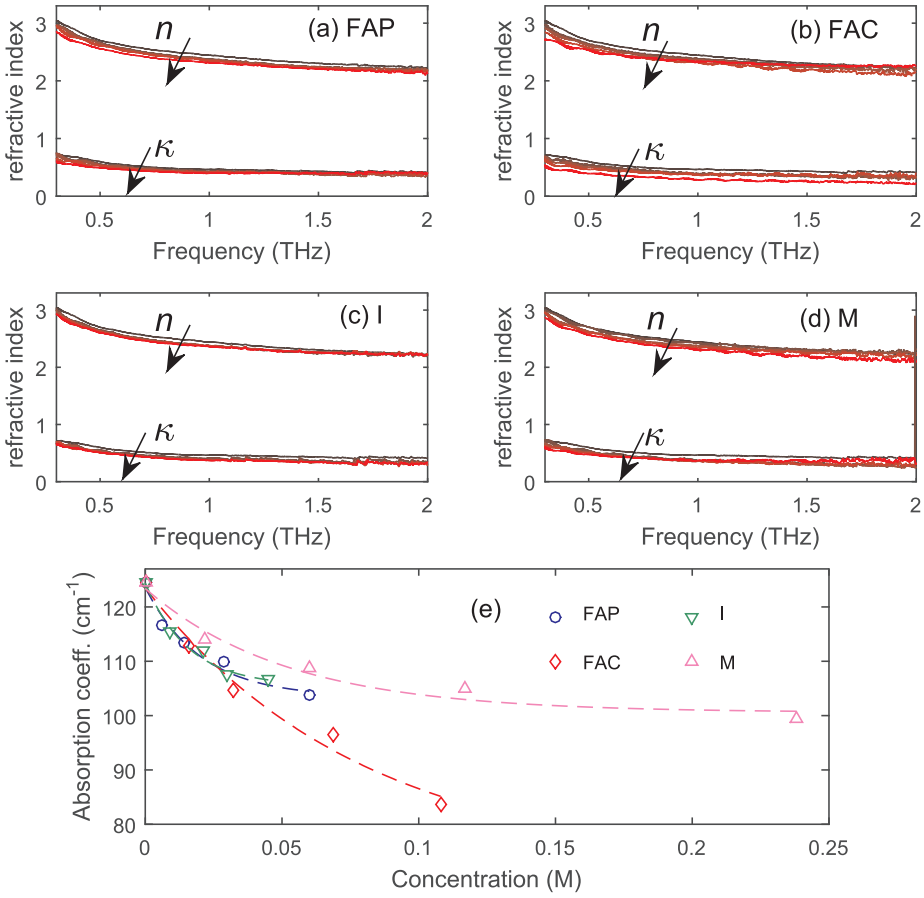


**Fig. 3.** (a), (b), (c) and (d) Variation of the complex refractive index with frequency at different carbohydrate concentrations in the aqueous solutions. The carbohydrate concentration increases from black to red as shown by arrows; (e) Variation of absorption coefficient (at 0.5 THz) with solute concentration in aqueous solutions. The absorption coefficient shows a non-proportional increase with decrease in the carbohydrate concentration. The dashed lines correspond a polynomial fits to the data. (For interpretation of the references to colour in this figure legend, the reader is referred to the web version of this article.)

frequency. A marginal decrease in magnitude with increasing solute concentrations was observed in all the aqueous solutions. To compare the hydration effect in all the carbohydrates studied here, the variation of absorption coefficient ($\alpha$) with the solute concentration at a particular test frequency of 0.5 THz is presented in Fig. 3(e). As shown in the figure, with increasing solute concentration absorption coefficient decreases, since the fraction of bulk water decreases while hydration water increases.

It is well known that the THz spectrum of pure water has contributions from many different modes. The slow relaxation mode (Shiraga et al., 2013, 2017, 2015) with peak frequency around 20 GHz is very sensitive to hydration, because the water molecules forming the hydration sphere are more restricted regarding their dynamics as compared to the bulk water. On the other hand, fast relaxation is less dependent on the hydration dynamics. In order to calculate the hydration number, we choose a characteristic frequency of 0.5 THz, given that this region is significant to hydration driven changes according to various models (Shiraga et al., 2013, 2017, 2015). The complex dielectric constant can be calculated from the refractive index. The hydration number of carbohydrate molecules in their aqueous solution can be calculated using the formula

$$n_h = N\frac{\epsilon''_{water}(0.5THz) - \epsilon''_{solution}(0.5THz)}{\epsilon''_{water}(0.5THz) - \epsilon''_{background}(0.5THz)} \quad (1)$$

where $N$ is the total number of water molecules per carbohydrate molecule, $\epsilon''_{water}$ (0.5 THz) is the imaginary part of the dielectric function of deionized water at 0.5 THz, $\epsilon''_{solution}$ (0.5 THz) is the one corresponding to the carbohydrate solution at 0.5 THz, and $\epsilon''_{background}$ (0.5 THz) corresponds to the fast relaxation of liquid water, which is known to be 0.95 at 0.5 THz (Shiraga et al., 2013). The dependence of the hydration number on the molarity of solute in the aqueous solution is shown in Fig. 4 for all the solutions studied here employing both techniques. It is clear from Fig. 4 that the hydration numbers extracted from THz spectroscopy are marginally higher than those extracted from the calorimetric study. The purified agave fructans have the highest hydration number followed by commercial agave fructans, inulin and maltodextrin, respectively. Commercial agave fructans show lower hydration as compared to purified agave fructans, given that commercial agave fructans contain a fraction of mono- and disaccharides as well. In addition, we estimated the hydration numbers for these carbohydrates employing ChemSketch (ACD labs, Toronto, Canada) software. The 3D structures of carbohydrates were optimized for Van der Waals forces in order to get the stable conformation. Based on the polarity observed at the different sites of the carbohydrates, the number of water molecules that a carbohydrate molecule may provide a site for were estimated thereafter, as shown in Fig. 5. The relative order of the hydration numbers of the carbohydrate estimated from the three methods are consistent. The estimated values of hydration number are shown in Table 1. The slight discrepancy between the calculated hydration numbers from the two experimental techniques may be attributed to their definition, which in a way correlated with the physical properties required for the hydration number calculation. For instance, the calorimetric method exploits the melting enthalpy measurement scheme and this static approach considers the water molecules strongly associated to the hydrophilic group of the macromolecule (Furuki, 2002), whereas, terahertz spectroscopy considers a dynamic approach and accounts for all the water molecules whose dynamics are slowed down by the presence of the macromolecule. In a very recent study by Charkhesht et al. (2018), the hydration shells of BSA proteins were classified as tightly bound water molecular layers and loosely bound water molecular layers, characterized by their relaxation times. Our computational estimation of the hydration number accounts for the first two hydration layers, which is in good agreement with that of the calorimetric values, as shown in Table 1. Comparing the calorimetric and

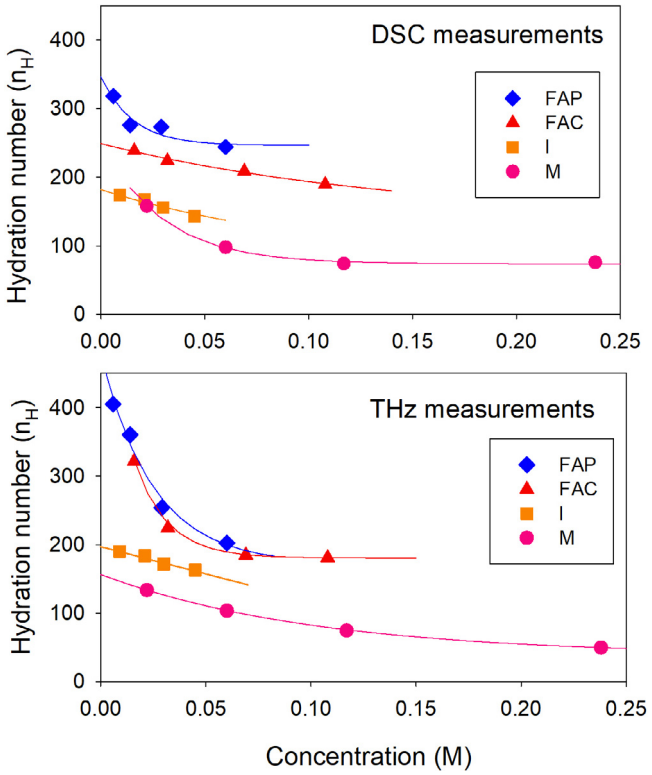


**Fig. 4.** Variation of the hydration number extracted from the calorimetric and terahertz data with solute concentration. The hydration number shows a non-proportional increase with decrease in the carbohydrate concentration. This behavior is more pronounced for the hydration numbers estimated from terahertz spectroscopy as compared to those estimated from the calorimetric method, as discussed in the text. The solid lines correspond the polynomial fits to the data.

computational estimation of hydration numbers, we conclude that the first two hydration layers encompass the tightly bound water molecules. The excess of hydration water molecules estimated by terahertz spectroscopy fall within the hydration shell but beyond the second layer, in the form of loosely bounded water molecules.

### 3.3. Characteristics of the hydration shells

In Figs. 3(e) and 4, we can see that with decreasing concentration of solute, the absorption coefficient and hydration number increase. However, it is to be noted that the absorption coefficient and hydration number per solute molecule are not proportional to the concentration of solute, as reported previously for mono- and disaccharides (Shiraga et al., 2013). The hydration number increases more rapidly with a decrease in solute concentration in the carbohydrate solutions. In this view, the recent work by Shiraga et al. (2017), on monosaccharides and disaccharides is noteworthy. In the first study of Shiraga et al. (2013), on disaccharides sucrose and maltose, the hydration number was reported to be increasing linearly with decreasing molar concentration up to 0.3 M in aqueous solution. However, in their latest research on sucrose and trehalose (Shiraga et al., 2017), they probe lower concentrations of the disaccharides in aqueous solutions, and it is clear from their study that the hydration number increases in a more rapid way below 0.3 M concentration as compared to the proportionality behavior observed up to 0.3 M concentration. The decrease in the hydration numbers with increasing solute concentration is consistent with overlapping of the hydration spheres around the solute molecules, which is expected for the concentrations we used. This is also consistent with recent publications (Charkhesht et al., 2018; Ebbinghaus et al., 2007) where Molecular Dynamics simulations demonstrate the overlapping of the hydration shells.

Furthermore, the influence of carbohydrates on water molecules in their vicinity can be classified as kosmotropic (Walrafen, 1966) (structure making) or chaotropic (Shiraga et al., 2015; Batchelor, Olteanu, Tripathy, & Pielak, 2004) (structure breaking). The kosmotropic behavior favors a hydrogen bond network identical to ice. As shown in Figs. 3(e) and 4, the rapid increase in absorption coefficient

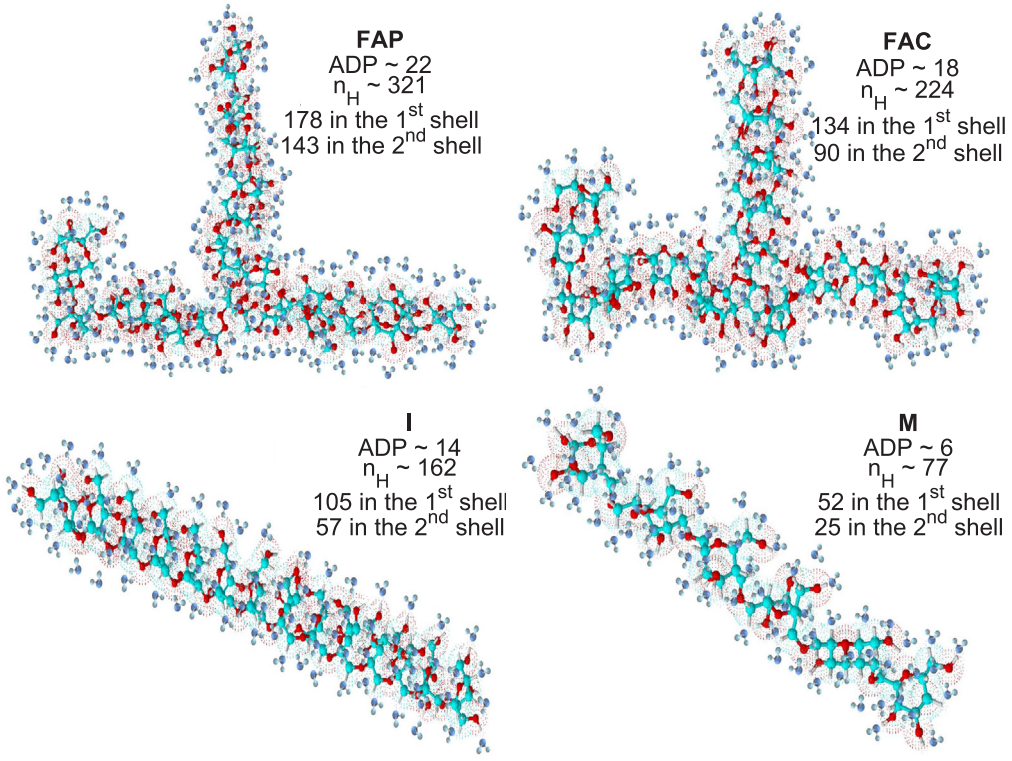


**Fig. 5.** The computational estimation of the hydration number for purified agave fructans (FAP), commercial agave fructans (FAC), inulin (I), and maltodextrin (M), employing the ChemSketch software. The estimated water molecules in the first two hydration layers are 321, 224, 162, and 77, for FAP, FAC, I, and M, respectively. ADP is abbreviation for the average degree of polymerization.

**Table 1**
Hydration numbers estimated from the differential scanning calorimetry, terahertz spectroscopy, and computational methods.

| Method | FAP | FAC | I | M |
|---|---|---|---|---|
| DSC | 318–224 | 239–190 | 174–143 | 158–76 |
| THz | 405–202 | 322–181 | 190–163 | 133–50 |
| Computational | 321 | 224 | 162 | 77 |

and hydration number as the carbohydrate concentration decreases reveals that with decreasing carbohydrate concentration, more water molecules are part of the hydration layers to form complex arrangements in the vicinity of the macromolecule. In this regard, Merzel and Smith (2002) predict, via molecular dynamics simulation on aqueous lysozyme solutions, that the density of water molecules in the first hydration layer is around 15 % higher as compared to that of the bulk water. They further propose a parallel alignment of water molecular dipoles induced by the electrostatic field of the macromolecule causing the higher density in the first hydration layer. Also, the potential of the macromolecule, to distort the H-bond network from bulk water, is expected to decrease with increasing distance from the macromolecule. Therefore, it appears less reasonable for all the hydration layers within the hydration shell to have an equal H-bond network. Such a behavior may not be explained considering an ice like H-bond network of water molecules in the vicinity of carbohydrate molecules, extending all the way from the first hydration layer to the end of the hydration sphere. Thus, in the context of our results, the chaotropic behavior appears to be more acceptable, where the presence of the macromolecule distorts the dynamical tetrahedral H-bond network and functions as a structure breaking agent. Similar arguments were put forth by Shiraga et al. (2013) and Shiraga et al. (2017) in their study on aqueous disaccharides in a significantly broad spectral range from 0.5 GHz to 12 THz by analyzing the damping constant and resonance frequency of -OH stretching vibrational motion occurring at around 5 THz, by fitting them to a model.

### 3.4. Comparison with trehalose as a hydrating agent and a bio-protectant

Another factor which plays a critical role for carbohydrates to behave as bio-protectants is their glass transition temperature. The glassy state is a dynamically frozen state with unusually high viscosity, as a result of which biomolecules become practically immobile and insulated from external stress (Jain & Roy, 2009). Among the disaccharides studied so far, trehalose is widely accepted as the very effective bio-protectant, and it has the highest glass transition temperature, around 390.15 K (Chen, Fowler, & Toner, 2000; Green & Angell, 1989). The carbohydrates studied here also fall on the high glass transition temperature side; for instance, agave fructans do at 391 K (Espinosa-Andrews & Rodríguez-Rodríguez, 2018; Espinosa-Andrews & Urias-Silvas, 2012), and inulin at 403 K (Espinosa-Andrews & Rodríguez-Rodríguez, 2018), which makes them good candidates to be used as bio-protectants. These carbohydrates are significantly larger than disaccharides such as trehalose and sucrose, and a rough comparison may be put forth regarding the hydration numbers of agave fructans, inulin and trehalose. The average molecular weights of agave fructans and inulin are 3539 g/mol and 2348 g/mol, respectively, whereas trehalose dihydrate is 378.3 g/mol. The molecular weight ratios of agave fructans and inulin to that of trehalose are around 9.4 and 8.5, respectively. The corresponding ratios of hydration number (extrapolated values at 0.10 M) are 8.75 (purified agave fructans) and 8.33 (commercial agave fructans) from THz measurements, and 11.25 (purified agave fructans) and 8.75 (commercial agave fructans) from calorimetric measurements. The comparison reveals that the hydration capacity of these fructans is closer to that of trehalose.

## 4. Conclusions

In summary, we present a study of the hydration shells of carbohydrates, namely, agave fructans, inulin, and maltodextrin, employing terahertz time-domain spectroscopy and differential scanning calorimetry. We extract the hydration number of the carbohydrates employing both techniques. The hydration numbers calculated from the terahertz spectroscopy are marginally higher than those of the calorimetric values. We attribute this discrepancy to the different analytical approaches adopted by the techniques. In our study, we conclude that the calorimetric estimation of the hydration shells corresponds the tightly bounded hydration molecules only, i.e., the first two hydration layers. The excess of hydration water molecules estimated by terahertz spectroscopy as compared to the calorimetric values designates the water molecules farther away in the hydration sphere, beyond the second hydration layer. In addition, the aqueous solutions show a non-linear increase in the absorption coefficient and the hydration number with decrease in the carbohydrates concentration. This behavior is attributed to the congregation of water molecules in the hydration layers to form complex arrangements. We demonstrate the non-proportional increase of the absorption coefficient and the hydration number as a characteristic of “chaotropic” or “structure breaking” model of the hydration shell around the carbohydrates.

We further compare the hydration ability of the agave fructans and inulin with that of trehalose via the ratio of their hydration number to the average molecular weight. We find that agave fructans and inulin may behave equivalently well regarding their hydration ability. With the high glass transition temperature and effective hydration ability, agave fructans and inulin maintain the characteristics of good bio-protectants and additives in food and beverages.

## Declaration of interests

None.

## Acknowledgements

The authors thank Dr. Lorena Moreno-Vilet, CONACYT- Centro de Investigación y Asistencia en Tecnología y Diseno del Estado de Jalisco, Mexico, for providing the purified agave fructans. The authors acknowledge the financial support of CONACYT through grants 252939, 255114, 280392, and 294440. The authors also thank to “FINNOVA CONACYT-SECRETARIA DE ECONOMÍA”. The authors are indebted to Mr. Mario Alberto Ruiz Berganza for English proofreading.

## References

Batchelor, J. D., Olteanu, A., Tripathy, A., & Pielak, G. J. (2004). Impact of protein denaturants and stabilizers on water structure. *Journal of the American Chemical Society, 126*(7), 1958–1961.
Beard, M. C., Turner, G. M., & Schmuttenmaer, C. A. (2002). Terahertz spectroscopy. *Journal of Physical Chemistry B, 106*(29), 7146–7159.
Born, B., Kim, S. J., Ebbinghaus, S., Gruebele, M., & Havenith, M. (2009). The terahertz dance of water with the proteins: the effect of protein flexibility on the dynamical hydration shell of ubiquitin. *Faraday Discussions, 141*, 161–173.
Branca, C., Magazù, S., Maisano, G., Migliardo, F., Migliardo, P., & Romeo, G. (2001). α, α-trehalose/water solutions. 5. hydration and viscosity in dilute and semidilute disaccharide solutions. *Journal of Physical Chemistry B, 105*(41), 10140–10145.
Cardoso, M. V., Carvalho, L. V., & Sabadini, E. (2012). Solubility of carbohydrates in heavy water. *Carbohydrate Research, 353*, 57–61.
Charkhesht, A., Regmi, C., Mitchell-Koch, K. R., Cheng, S., & Vinh, N. Q. (2018). High-precision megahertz-to-terahertz dielectric spectroscopy of protein collective motions and hydration dynamics. *Journal of Physical Chemistry B*.
Chen, T., Fowler, A., & Toner, M. (2000). Literature review: Supplemented phase diagram of the trehalose–water binary mixture. *Cryobiology, 40*(3), 277–282.
Cipcigan, F., Sokhan, V., Martyna, G., & Crain, J. (2018). Structure and hydrogen bonding at the limits of liquid water stability. *Scientific Reports, 8*(1), 1718.
Contreras-Haro, B., Robles-Cervantes, J. A., Gonzalez-Ortiz, M., Martinez-Abundis, E., Espinel-Bermudez, C., Gallegos-Arreola, M. P., & Morgado-Castillo, K. C. (2017). The effect of agave tequilana weber inulin on postprandial ghrelin concentration in obese patients. *Journal of Medicinal Food, 20*(2), 197–199.

Ebbinghaus, S., Kim, S. J., Heyden, M., Yu, X., Heugen, U., Gruebele, M., ... Havenith, M. (2007). An extended dynamical hydration shell around proteins. *Proceedings of the National Academy of Sciences of the United States of America, Vol. 104*(52), 20749–20752.

Engelsen, S., Herve du Penhoat, C., & Perez, S. (1995). Molecular relaxation of sucrose in aqueous solutions: How a nanosecond molecular dynamics simulation helps to reconcile nmr data. *The Journal of Physical Chemistry, 99*(36), 13334–13351.

Espinosa-Andrews, H., & Rodríguez-Rodríguez, R. (2018). Water state diagram and thermal properties of fructans powders. *Journal of Thermal Analysis and Calorimetry, 132*(1), 197–204.

Espinosa-Andrews, H., & Urias-Silvas, J. E. (2012). Thermal properties of agave fructans (agave tequilana weber var. azul). Carbohydrate. *Polymer, 87*(4), 2671–2676.

Furuki, T. (2002). Effect of molecular structure on thermodynamic properties of carbohydrates. a calorimetric study of aqueous di-and oligosaccharides at subzero temperatures. *Carbohydrate Research, 337*(5), 441–450.

Galema, S. A., & Hoeiland, H. (1991). Stereochemical aspects of hydration of carbohydrates in aqueous solutions. 3. Density and ultrasound measurements. *J. Physical Chemistry, 95*(13), 5321–5326.

García-Vieyra, M. I., Del Real, A., & López, M. G. (2014). Agave fructans: their effect on mineral absorption and bone mineral content. *Journal of Medicinal Food, 17*(11), 1247–1255.

Green, J. L., & Angell, C. A. (1989). Phase relations and vitrification in saccharide-water solutions and the trehalose anomaly. *The Journal of Physical Chemistry, 93*(8), 2880–2882.

Guo, N., Puhlev, I., Brown, D. R., Mansbridge, J., & Levine, F. (2000). Trehalose expression confers desiccation tolerance on human cells. *Nature Biotechnology, 18*(2), 168.

Head-Gordon, T., & Johnson, M. E. (2006). Tetrahedral structure or chains for liquid water. *Proceedings of the National Academy of Sciences of the United States of America, 103*(21), 7973–7977.

Heugen, U., Schwaab, G., Bründermann, E., Heyden, M., Yu, X., Leitner, D., & Havenith, M. (2006). Solute-induced retardation of water dynamics probed directly by terahertz spectroscopy. *Proceedings of the National Academy of Sciences of the United States of America, 103*(33), 12301–12306.

Jain, N. K., & Roy, I. (2009). Effect of trehalose on protein structure. *Protein Science, 18*(1), 24–36.

Knab, J., Chen, J.-Y., & Markelz, A. (2006). Hydration dependence of conformational dielectric relaxation of lysozyme. *Biophysical Journal, 90*(7), 2576–2581.

Lipps, F., Levy, S., & Markelz, A. (2012). Hydration and temperature interdependence of protein picosecond dynamics. *Physical Chemistry Chemical Physics, 14*(18), 6375–6381.

López-Romero, J. C., Ayala-Zavala, J. F., González-Aguilar, G. A., Peña-Ramos, E. A., & González-Ríos, H. (2017). Biological activities of agave by-products and their possible applications in food and pharmaceuticals. *Journal of the Science of Food and Agriculture, 98*(7), 2461–2474.

Magno, A., & Gallo, P. (2011). Understanding the mechanisms of bioprotection: a comparative study of aqueous solutions of trehalose and maltose upon supercooling. *Journal of Physical Chemistry Letters, 2*(9), 977–982.

Merzel, F., & Smith, J. C. (2002). Is the first hydration shell of lysozyme of higher density than bulk water? *Proceedings of the National Academy of Sciences of the United States of America, 99*(8), 5378–5383.

Moreno-Vilet, L., Bostyn, S., Flores-Montano, J.-L., & Camacho-Ruiz, R.-M. (2017). Size-exclusion chromatography (hplc-sec) technique optimization by simplex method to estimate molecular weight distribution of agave fructans. *Food Chemistry, 237*, 833–840.

Rossi, B., Comez, L., Fioretto, D., Lupi, L., Caponi, S., & Rossi, F. (2011). Hydrogen bonding dynamics of cyclodextrin–water solutions by depolarized light scattering. *Journal of Raman Spectroscopy, 42*(6), 1479–1483.

Sajadi, M., Ajaj, Y., Ioffe, I., Weingärtner, H., & Ernsting, N. P. (2010). Terahertz absorption spectroscopy of a liquid using a polarity probe: a case study of trehalose/water mixtures. *Angewandte Chemie International Edition, 49*(2), 454–457.

Sajadi, M., Berndt, F., Richter, C., Gerecke, M., Mahrwald, R., & Ernsting, N. P. (2014). Observing the hydration layer of trehalose with a linked molecular terahertz probe. *Journal of Physical Chemistry Letters, 5*(11), 1845–1849.

Sáyago-Ayerdi, S. G., Mateos, R., Ortiz-Basurto, R. I., Largo, C., Serrano, J., Granado-Serrano, A. B., ... Tabernero, M. (2014). Effects of consuming diets containing agave tequilana dietary fibre and jamaica calyces on body weight gain and redox status in hypercholesterolemic rats. *Food Chemistry, 148*, 54–59.

Shiraga, K., Adachi, A., Nakamura, M., Tajima, T., Ajito, K., & Ogawa, Y. (2017). Characterization of the hydrogen-bond network of water around sucrose and trehalose: Microwave and terahertz spectroscopic study. *The Journal of Chemical Physics, 146*(10), 105102 .

Shiraga, K., Ogawa, Y., Kondo, N., Irisawa, A., & Imamura, M. (2013). Evaluation of the hydration state of saccharides using terahertz time-domain attenuated total reflection spectroscopy. *Food Chemistry, 140*(1–2), 315–320.

Shiraga, K., Suzuki, T., Kondo, N., De Baerdemaeker, J., & Ogawa, Y. (2015). Quantitative characterization of hydration state and destructuring effect of monosaccharides and disaccharides on water hydrogen bond network. *Carbohydrrate Research, 406*, 46–54.

Singh, A. K., Morales, J. A., Estrada, N. A., Rodriguez, S. J. V., & Castro-Camus, E. (2018). Terahertz hydration dynamics in aqueous polysaccharides. *2018 43rd International Conference on Infrared, Millimeter, and Terahertz Waves (IRMMW-THz)*(pp. 1–2). IEEE.

Soltani, A., Jahn, D., Duschek, L., Castro-Camus, E., Koch, M., & Withayachumnankul, W. (2016). Attenuated total reflection terahertz time-domain spectroscopy: uncertainty analysis and reduction scheme. *IEEE Transactions on Terahertz Science and Technology, 6*(1), 32–39.

Walrafen, G. (1966). Raman spectral studies of the effects of urea and sucrose on water structure. *The Journal of Chemical Physics, 44*(10), 3726–3727.